

Static fatigue and time to failure predictions of particulate filled epoxide resin composites

H. R. BEER, T. KAISER

Zentrallabor, Ress. Kunststoffe und Keramik, Brown Boveri and Cie. AG, Postfach, CH-8050 Zürich, Switzerland

A. C. MOLONEY, H. H. KAUSCH

Laboratoire de Polymères, Ecole Polytechnique Fédérale de Lausanne, Ch. de Bellerive 32, 1007 Lausanne, Switzerland

The long term strength of two composites under constant load has been measured at various temperatures during a period of up to 2 years. Based on the concepts of linear elastic fracture mechanics, times to failure were predicted from short term experiments. The parameters necessary for the analysis were determined using either the double torsion test technique or by measurements of tensile strength at constant stressing rates. It has been found that both procedures lead to nearly equivalent predictions of the static fatigue behaviour of laboratory specimens from room temperature almost up to the glass transition temperature. Deviation of the predictions from experimental long term data are minor and are thus well acceptable for engineering design.

1. Introduction

In medium and high voltage insulation applications particulate filled polymers are widely used. Examples are various kinds of post and support insulators, bushings, cable terminals, instrument transformers and circuit breakers (including pressure vessels). In general these are indoor applications. However, tendencies exist to develop special polymers for outdoor insulation as possible substitutes for porcelain.

Epoxide resins with silica or alumina flour as fillers are principally used in this field. These composites are brittle, due to the high crosslink density of the organic matrix and the brittleness of inorganic fillers. One dominant feature of their brittleness is that they exhibit a distinct time dependence of strength. Besides electrical stress, insulators are also subjected to notable static mechanical stress. It is therefore essential in engineering design to know the long term strength behaviour of the epoxide resin composites. During the past decade techniques for lifetime predictions based on short time experiments have been developed for another class of brittle materials: ceramics. An excellent review on this topic was given by Pletka and Wiederhorn [1]. The time dependence of strength, also known as static fatigue, is explained as follows: technical parts are subject to inherent flaws such as pores, inhomogeneities, cracks, notches etc. that result from the manufacturing or machining process. The flaws are starting points for cracks that begin to develop and grow under mechanical stress. Cracks propagate at stresses far below the short term strength of the material. During this phase of slow subcritical crack growth technical parts may remain in operation without exhibiting any external signs of damage. When the crack has reached a critical size its propagation velocity increases sharply. As a conse-

quence sudden failure of the sample occurs. The lifetime of a technical part is therefore mainly determined by the phase of subcritical crack growth. The fracture mechanics concept has been proven to be useful for the quantitative understanding of crack growth behaviour. This theory provides a basis to describe crack propagation as a function of the stress field around the crack tip. This enables the prediction of long term strength with parameters measured by short time experiments. Several experimental techniques exist for the determination of these crack growth parameters see [1-3].

Failure predictions in the manner described above have meanwhile reached the state of the art for ceramics. However, only a few attempts of applying this approach to polymers have been reported. Beaumont and Young [4] and Döll and Könczöl [5] obtained lifetime predictions for polymethylmethacrylate (PMMA) based on double torsion experiments that correlate well with measured long term data. Different findings have been achieved for epoxide resins and their composites. For an epoxide resin reinforced with aramid fibres a good correlation between prediction and long term experiment has been found [6]. In an investigation on an epoxide resin with an intermediate level of particulate filler deviations of the calculated predictions from the static fatigue data are only negligible within a period of 60 days measuring time [7].

Some controversial results have been found concerning the long term behaviour of unfilled epoxide resins under constant load. There is some evidence that these materials are not subject to static fatigue [8-10]. However, previous investigations carried out in our laboratory on unfilled epoxides cured with various types of amine hardeners revealed a distinct

time dependence of tensile strength [11]. The aim of the present work was to examine the applicability of life time prediction techniques to epoxide resins with very high filler loadings (up to 60 vol %).

2. Theory

At room temperature the materials investigated exhibit only negligible deviations from ideal elastic behaviour. It is therefore justified to use linear elastic fracture mechanics (LEFM) as a basis for failure predictions. The central quantity in LEFM is the stress intensity factor K . In crack opening mode I K_I describes the stress field around the crack tip as imposed by the external stress σ

$$K_I = \sigma f a^{1/2} \quad (1)$$

where a is the crack length and f is a geometrical factor dependent on crack shape, specimen shape and loading. In order to quantify the load dependent crack growth, it is necessary to find a relation between crack growth velocity $v = da/dt$ and stress intensity factor. In practice the empirical power law

$$v = AK_I^n \quad (2)$$

has proved to describe the relationship in question with sufficient accuracy. A and n are environmentally dependent quantities.

On differentiating Equation 1 with respect to time ($\sigma = \text{constant}$) and substituting in Equation 2 for v it is possible to express time to failure, i.e. the lifetime t_L as follows

$$t_L = 2/(\sigma^2 f^2 A) \int_{K_{II}}^{K_{Ic}} K_I^{1-n} dK_I \quad (3)$$

Integration is carried out between the limits K_{II} (stress intensity factor at the most dangerous initial flaw of size a_i) and K_{Ic} (critical stress intensity factor at which crack propagation accelerates precipitously). After integration, introducing some reasonable simplifications and expressing K_{II} by S_i

$$K_{II} = K_{Ic} \sigma / S_i \quad (4)$$

where S_i is the fracture strength when no subcritical crack growth occurs prior to failure, the time to failure can be calculated according to Equation 5:

$$t_L = [1/2f^2 AK_{Ic}^{n-2}(n-2)]^{-1} (S_i^{n-2} \sigma^{-n}) \quad (5)$$

Equation 5 signifies that the lifetime depends on the externally applied stress σ as the only variable. Several experimental techniques exist to determine all other parameters in Equation 5.

From long term experiments, where the time to failure of a set of specimens is recorded as a function of the applied constant stress, a global constant

$$C_1 = [1/2f^2 AK_{Ic}^{n-2}(n-2)]^{-1} S_i^{n-2} \quad (6)$$

and n can be determined:

$$t_L = C_1 \sigma^{-n} \quad (7)$$

In a double logarithmic plot of the stress/failure time data, a linear regression analysis yields the parameters of a straight line with slope $-n$ and intercept $\log(C_1)$.

The parameters of constant $C_2 = [1/2f^2 AK_{Ic}^{n-2}(n-2)]^{-1}$ can be determined from measurements of

crack velocity as a function of stress intensity factor in double torsion experiments. The lifetime equation becomes in this case

$$t_L = C_2 S_i^{n-2} \sigma^{-n} \quad (8)$$

S_i has to be evaluated from separate strength measurements. Evans [12] has described a means to obtain values for C_2 and n from short time strength measurements. For this purpose it is necessary to determine the strength S at different constant stressing rates $d\sigma/dt$ according to Equation 9:

$$S^{n+1} = C_2(n+1) S_i^{n-2} d\sigma/dt \quad (9)$$

A double logarithmic plot of S against $d\sigma/dt$ yields n as the slope and C_2 from the intercept of the line of best fit.

3. Experimental details

All experiments have been carried out with two composites. Composite A was a trifunctional hydantoin resin (XB 2818A) cured with hexahydrophthalic anhydride (HT 907) and filled to 60 vol % with a mixture of alumina flour (Starck and Co.) and silane treated glass beads (Ballotini 2227 CP03). Composite B was a formulated resin (XB 2900) cured with a modified anhydride hardener (HY 925) and filled to 41 vol % with silica flour (Quarzwerte Frechen). Resins and curing agents were products of Ciba-Geigy. The components were mixed at 80°C. The mixture was then pre-evacuated, poured into steel moulds, evacuated and cured in the moulds at 160°C for 16 h.

Tensile strength measurements were conducted on an Instron 1195 testing machine equipped with a heating chamber. Experiments were carried out on shoulder bars with rectangular cross section (4 mm × 10 mm) with a usable length of 65 mm; at crosshead speeds between 0.05 and 500 mm min⁻¹.

Static fatigue was measured with simple loading devices as shown in Fig. 1, which were placed into ovens for experiments at elevated temperatures. The samples consisted of short shoulder bars 4 mm × 10 mm with a usable length of 30 mm. Part of the fatigue data was collected in heatable creep testing

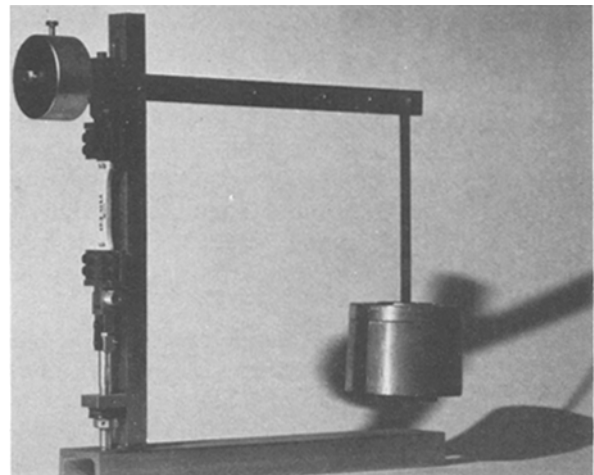


Figure 1 Loading device for static fatigue experiments with short shoulder bars.

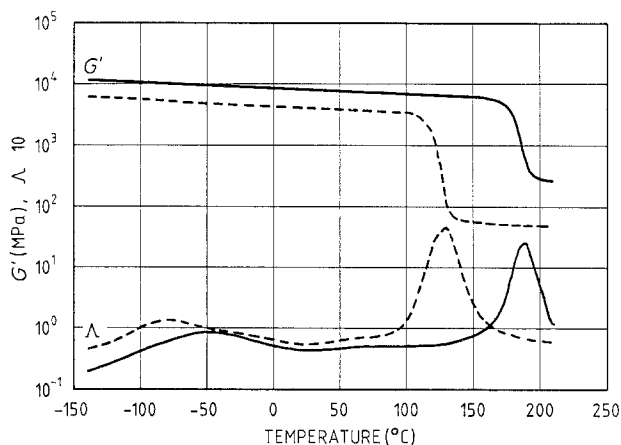


Figure 2 Shear modulus (G') and logarithmic decrement of mechanical damping (Δ) of composites A (—) and B (---) as function of temperature.

machine (Karl Frank GmbH) on shoulder bars with square cross-section (10 mm \times 10 mm) and a usable length of 60 mm. Crack speed/stress intensity factor data were determined by the double torsion technique [13]. Samples of dimensions 34 mm \times 30 mm \times 80 mm were cut from moulded plates and a groove (0.5 to 1 mm) was machined on the tensile side by means of a milling tool. Crack growth velocities in the range 10^{-1} to 10^{-8} m sec $^{-1}$ could be measured by the graphite spray technique described elsewhere [14]. Data were collected in the constant displacement rate mode at crosshead speeds 0.05 to 0.2 mm min $^{-1}$ and in the load relaxation mode [2].

All measurements were conducted in air, for composite A at 23, 120 and 180°C, for composite B at 23, 85 and 105°C. Temperatures of 120 and 85°C, respectively, are typical working values for technical parts made of these materials. However, temperatures of 180 and 105°C, respectively, are close to the glass transition temperature, i.e. at the beginning of the transition from the energy-elastic to the entropy-elastic state. The thermomechanical properties of the two composites are illustrated by the shear modulus/temperature curves shown in Fig. 2 (recorded on a Brabender torsion pendulum).

4. Results and discussion

4.1. Strength measurements

Schematic stress-strain curves for composites A and B in tensile loading are represented in Fig. 3. This diagram confirms the brittleness of the two materials at room temperature; the behaviour is almost ideally linear elastic. The elongation at break of 0.3% for composite A is remarkably low for a polymeric material. The deviations from linearity are somewhat more distinct at the typical working temperatures 120°C (A) and 85°C (B). However, viscoelastic contributions only gain greater importance at the extreme temperatures where sometimes yielding before break was observed (180°C for composite A and 105°C for composite B). Figs 4 and 5 show tensile strength measurements at different strain rates. The testing machine employed was displacement controlled and thus stressing rates $d\sigma/dt$ had to be approximated

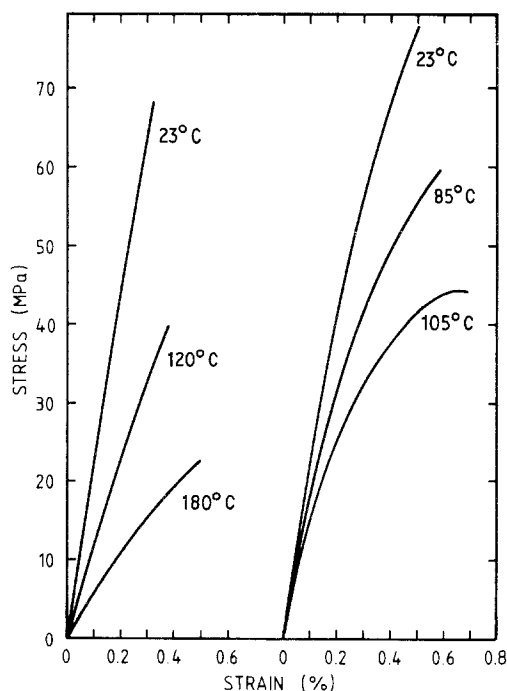


Figure 3 Stress-strain curves up to failure of composites A (left) and B (right) at various temperatures.

from strain rates $d\epsilon/dt$ by Equation 10

$$d\sigma/dt = E d\epsilon/dt \quad (10)$$

where E is Young's modulus. The justification for this approximation was derived from the above mentioned quasi-linear elastic behaviour of the materials investigated. The error bars represent standard deviations for ten specimens at each measuring point.

Crack growth parameters n and C_2 were determined from a linear regression analysis of a double logarithmic plot of strength values against stressing rates. S_i is represented as the mean strength at the highest stressing rate. Table I gives a summary of the strength measurements data.

4.2. Crack growth measurements

Crack velocity measurements as a function of stress intensity factor are illustrated in Figs 6 and 7. The double torsion technique in combination with conductivity measurements of a graphite layer on the specimen allowed to record crack velocities ranging from 10^{-1} to 10^{-8} m sec $^{-1}$. Most of the data were obtained using the load relaxation method [2]. Some of the data around crack propagation speeds of 10^{-4} m sec $^{-1}$ were collected by the constant displacement rate technique. The load-time curves of the latter experiments revealed stable crack propagation in all cases. No stick-slip behaviour was observed.

TABLE I Summary of strength measurements

	Temperature (°C)	S_i (MPa)	n	$\log C_2$
Composite A	23	73.4	35.8	2.68
	120	50.0	14.7	2.37
	180	27.1	11.8	2.55
Composite B	23	86.8	34.7	2.79
	85	72.6	22.8	2.87
	105	63.9	13.2	2.79

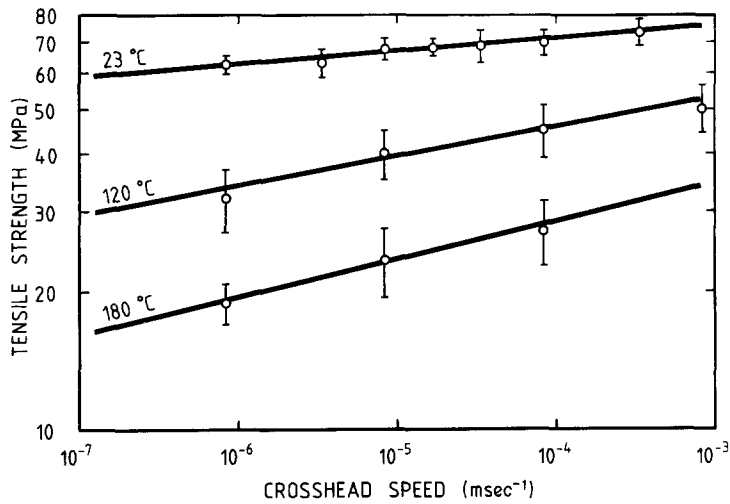


Figure 4 Tensile strength as a function of crosshead displacement rate at different temperatures for composite A.

In the double logarithmic plots the data fit well to a straight line at the two lower temperatures. This means that the empirical Equation 2 represents a good description of the relation between crack velocity and stress intensity factor. The crack growth parameters n and A could therefore be obtained from the slope and the intercept of the regression lines (straight lines in Figs 6 and 7).

This simple relationship no longer holds for both composites at their respective extreme temperatures. Clearly two crack growth ranges can be distinguished. In each range the data points are linearly related. The existence of different regimes of crack growth is well known for ceramics exposed to stress corrosive environments. For those materials they are explained by different chemical reaction mechanisms that control crack propagation. However, a similar explanation is not applicable to the present study since measurements under discussion were conducted in air at 105 and 180 °C, that is in a non-corrosive atmosphere. The explanation has to be sought in the viscoelastic contributions at these temperatures. According to Findley [15] the time dependent deformation $\varepsilon(t)$ of polymers can be described by Equation 11

$$\varepsilon(t) = \varepsilon_0 + \varepsilon_x t^q \quad (11)$$

where ε_0 is the initial linear elastic deformation and the exponential term with the empirical constants ε_x and q

characterizes the viscoelastic deformation. While at the lower temperatures the viscoelastic contributions are negligibly small they have to be taken into account at 180 and 105 °C for composites A and B, respectively. On initially loading the double torsion specimen in relaxation measurements, linear elastic fracture behaviour is observed. This region is represented by the steeper part of the $v(K_I)$ curve (see Figs 6c and 7c). After a certain time — determined by the exponential term of Equation 11 — viscoelastic behaviour becomes dominant and the slope of the $v(K_I)$ curve decreases markedly. Lifetime predictions according to Section 2 are based on linear elastic fracture mechanics. It is clear that this concept in its strict sense is not applicable in the non-linear region. Nevertheless we tried to apply the LEFM concept for failure predictions at the high temperatures, bearing in mind that this would yield only approximate results. For this purpose only crack growth data of region I of the high temperature curves in Figs 6 and 7 were taken into account. Crack propagation parameters were obtained from the estimated fits (region I lines in Figs 6 and 7). Table II gives a summary of the crack growth parameters determined from double torsion measurements.

4.3. Static fatigue and lifetime predictions

Long term strength measurements are illustrated in

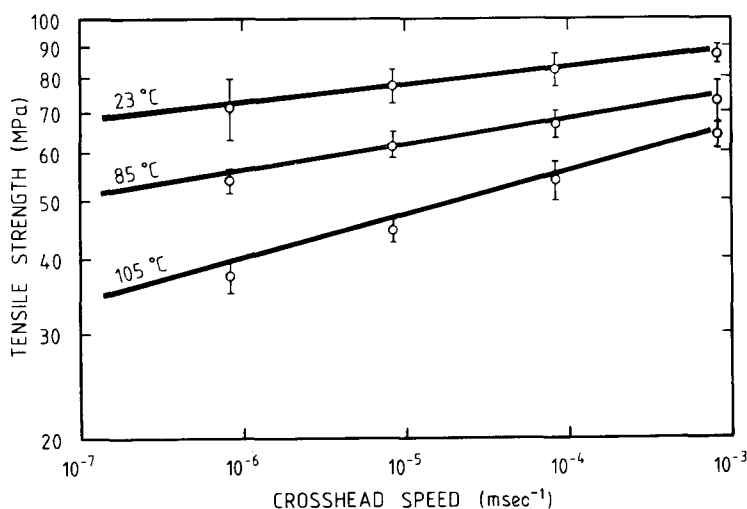


Figure 5 Tensile strength as a function of crosshead displacement rate at different temperatures for composite B.

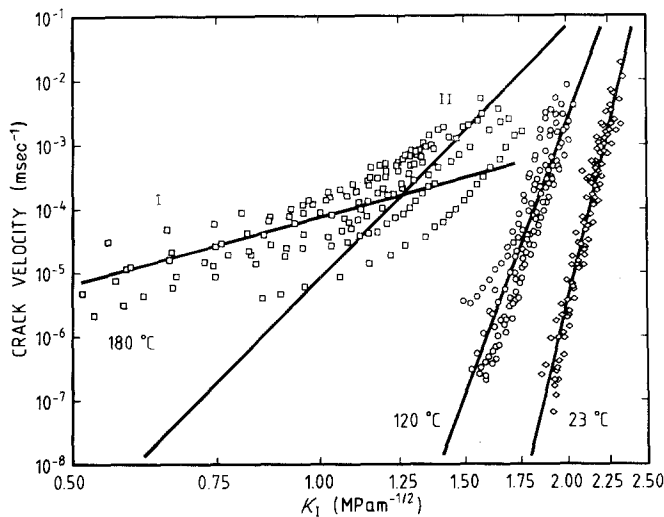


Figure 6 Crack velocity as a function of stress intensity factor for composite A as obtained by the double torsion technique. Data points represent values from load relaxation and constant displacement rate experiments; (—) line of best fit obtained from regression analysis.

Figs 8 and 9 at various temperatures. Each data point represents an individual specimen. The dotted fracture line was calculated by linear regression analysis. The corresponding parameters n and C_1 are given in Table III. Shaded areas indicate the 95% confidence band along the fracture line.

Some discrepancies are noted concerning the crack growth exponent n , which determines the slope of the fracture line. For resin B, n is steadily decreasing with increasing temperature. However, for resin A, n reaches a maximum value at 120°C. It has to be assumed that this singularity emerges from the experimental procedure. Data for resin A at 120°C were collected from different equipment and specimen shapes. This led to a considerable scatter of data, resulting in a poor correlation coefficient of 0.75 in the regression analysis. The correlation coefficients of the other sets of long term measurements are above 0.94. The n values determined from double torsion experiments or from constant stressing rate measurements are steadily decreasing with increasing temperature for both composites. Therefore we assume that the n value of 49.5 for composite A at 120°C is in fact too high. In analogy to the other sets of experiments it should lie between 8.9 and 25.7 (see Table III).

Figs 8 and 9 clearly indicate that the two composites are subject to static fatigue within the temperature regions investigated. In all six sets of measurements no change in slope of the fracture line is

observed. This suggests that failure mechanisms remained unaltered during the entire period studied experimentally.

On the basis of double torsion and constant stressing rate measurements lifetime predictions have been calculated for composites A and B at each experimental temperature. Besides the crack growth exponent n , at least one of the interdependent quantities a_i , S_i or K_{Ic} has to be evaluated for the computations. Since there are experimental difficulties in determining exact values of the latter three quantities, Döll and Könczöl's procedure [5] has been adopted in the present work. This method consists of combining a short static fatigue experiment with crack growth data from double torsion experiments. The lifetime predictions presented in this paper were calculated by combining the long term strength at $t = 10^5$ sec with the slope determining n value from either constant stressing rate experiments or from double torsion data. These are illustrated by the straight and dashed lines in Figs 8 and 9. The validity of the predictions is estimated by comparison with the experimentally determined strength under static load. In general both prediction procedures are in satisfactory agreement with the long term experiments.

Almost all predictions tend to be slightly optimistic. However, extrapolations on the time scale by one decade beyond the longest measuring time result in deviations of only a few per cent on the stress scale.

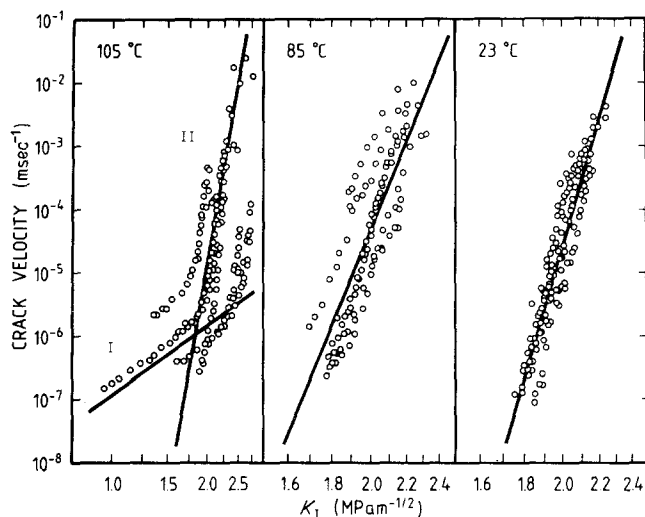


Figure 7 Crack velocity as a function of stress intensity factor for composite B as obtained by the double torsion technique. Data points represent values from load relaxation and constant displacement rate experiments; (—) line of best fit obtained from regression analysis.

TABLE II Summary of crack growth measurements

	Temperature (°C)	K'_{Ic} (MPa m ^{-1/2})	n	log A
Composite A	23	2.35 ¹	49.9	-20.5
	120	2.05 ¹	34.3	-13.0
	180	1.25 ²	3.5	-4.2
Composite B	23	2.25 ¹	48.0	-19.0
	85	2.25 ¹	33.6	-14.4
	105	1.80 ²	3.9	-6.7

¹The $v(K_I)$ curves do not exhibit any characteristic change in slope, which would allow the definition of a distinct K_{Ic} value. Therefore the highest measured data point was used in calculations as an approximate K'_{Ic} value. The fracture toughness of composite A at room temperature determined by the single edge notch (SEN) technique was 2.325 MPa m^{-1/2}. This differs only slightly from our K'_{Ic} value, thus justifying the foregoing procedure.

² K'_{Ic} at the extreme temperatures corresponds to transition from region I to region II in Figs 6 and 7.

Such minor deviations are acceptable in engineering design, since these extrapolations cover the range between 10 and 20 years.

It is not surprising that predictions made from constant stressing rate experiments lie somewhat closer to the static fatigue data than predictions using double torsion data. In the latter specimen geometry

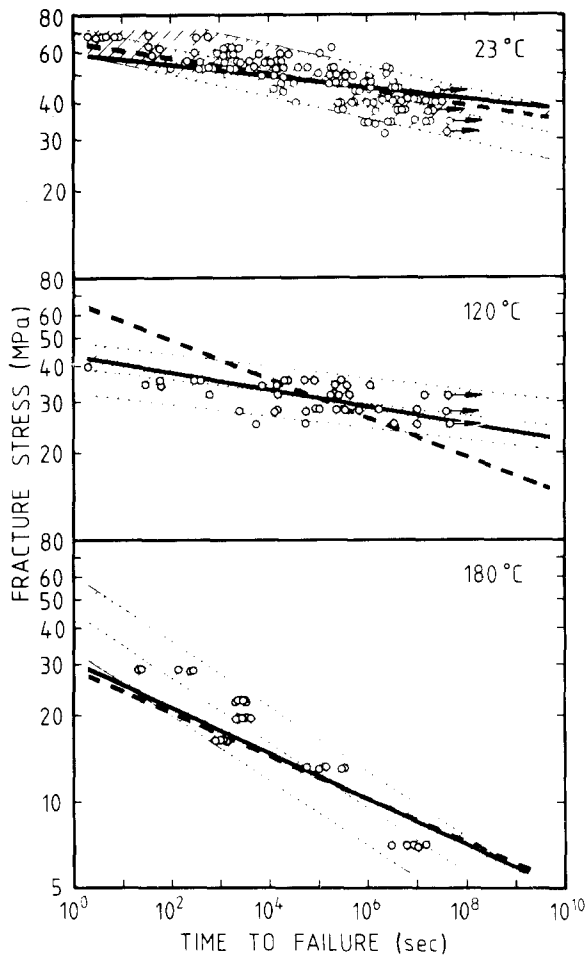


Figure 8 Static fatigue and life time predictions of composite A at various temperatures; (O) fracture time/fracture stress of individual specimens; (→) specimen not broken, experiment interrupted; (.....) fracture line obtained from regression analysis, with 95% confidence band (shaded area); (—) prediction using parameters determined from double torsion experiments; (---) predictions using parameters determined from constant stressing rate experiments.

TABLE III Summary of long term strength measurements

	Temperature (°C)	n	log C_1
Composite A	23	25.7	48.0
	120	49.5	79.0
	180	8.9	14.8
Composite B	23	28.8	65.1
	85	23.8	44.9
	105	14.6	26.7

a single macrocrack is forced to propagate along a guided path whereas in the former two experiments a smooth sample is uniformly stressed, thus invoking the initiation of one or several cracks throughout the entire volume of the specimen. However, the fact that the fracture mechanics DT-experiment provides a good description of the static fatigue experiments implies that the lifetime of a sample under constant load is indeed determined by the growth of one single microcrack. This still holds when the material deviates from linear elastic behaviour (cf. Fig. 3). The temperature where samples begin to yield in the tensile strength experiment marks an extreme of the applicability range for lifetime predictions based on LFM.

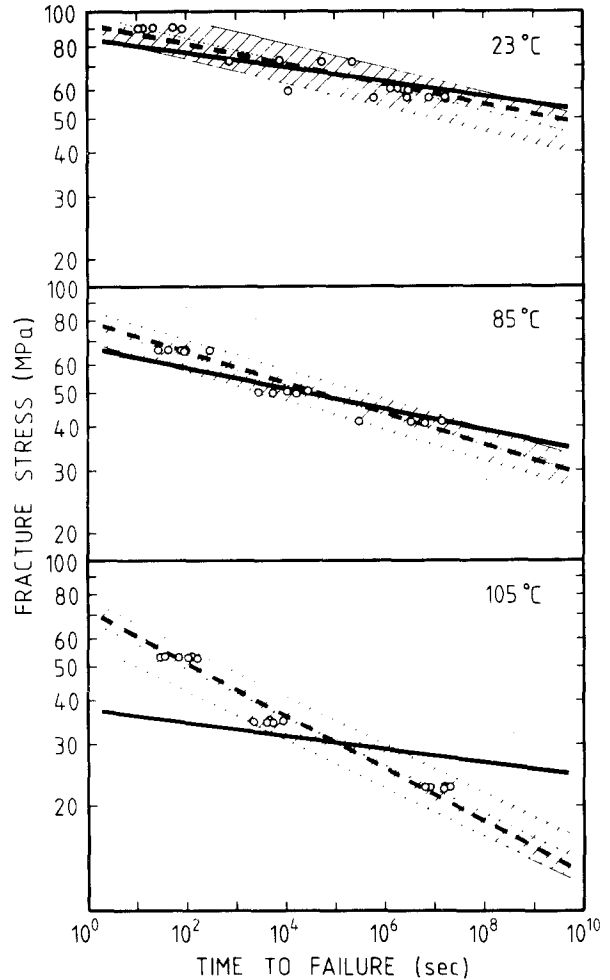


Figure 9 Static fatigue and lifetime predictions of composite B at various temperatures; (O) fracture time/fracture stress of individual specimens; (.....) fracture line obtained from regression analysis, with 95% confidence band (shaded area); (—) prediction using parameters determined from double torsion experiments; (---) predictions using parameters from constant stressing rate experiments.

This is the case for composite B at 105°C. In fact, at this temperature the fracture mechanics experiment understandably leads to a considerable misfit between predictions and long term experiments.

The physical meaning of the initial flaw size a_i remains an unanswered question. Calculations in this work yielded values for a_i between 100 and 500 μm , i.e. dimensions where a flaw should be detectable by the naked eye. Fracture surface morphologies indicate that fracture starts usually at edges of the square or rectangular specimens. However, no cracks have ever been detected before fracture in the long term experiments.

A more detailed discussion concerning the meaning of the "inherent flaw size", accompanied by fractographic investigations will be given in [16].

Strength and fracture time data exhibit considerable scatter. Treatment of this scatter with statistical methods will be presented in a separate publication [17].

5. Conclusions

Particulate filled epoxide resins are subject to static fatigue — a fact that must be accounted for in engineering design.

The time dependent strength of laboratory specimens under constant load can be predicted on the basis of the fracture mechanics crack growth model.

Material parameters needed for the calculation of lifetime predictions may be determined by crack growth measurements in double torsion specimens or by constant stressing rate experiments on smooth tensile specimens. Both techniques provide almost equivalent predictions that are in satisfactory agreement with static fatigue data.

On the basis of these experimental results we can suggest a procedure for long term strength predictions that is based on a short term static fatigue experiment with an expected time to failure of between 1 and

10 days. An extrapolation may then be made beyond these experimental times using crack growth parameters determined from constant stressing rate experiments. This provides the engineer with predictions of lifetime under constant load that have sufficient accuracy.

References

1. B. J. PLETKA and S. M. WIEDERHORN, *J. Mater. Sci.* **17** (1982) 1247.
2. A. G. EVANS, *ibid.* **7** (1972) 1137.
3. R. W. DAVIDGE, "Mechanical Behaviour of Ceramics" (Cambridge University Press, Cambridge, 1979) p. 39.
4. P. W. R. BEAUMONT and R. J. YOUNG, *J. Mater. Sci.* **10** (1985) 1134.
5. W. DÖLL and L. KÖNCZÖL, *Kunststoffe* **70** (1980) 9.
6. R. M. CHRISTENSEN and R. E. GLASER, *J. Appl. Mech.* **52** (1985) 1.
7. R. J. YOUNG and P. W. R. BEAUMONT, *J. Mater. Sci.* **10** (1975) 1343.
8. J. O. OUTWATER and D. J. GERRY, *J. Adhesion* **1** (1969) 290.
9. D. C. PHILLIPS, J. M. SCOTT and M. JONES, *J. Mater. Sci.* **13** (1978) 311.
10. R. A. GLEDHILL, A. T. KINLOCH and S. J. SHAW, *ibid.* **14** (1979) 1769.
11. J. KAISER, Zentrallabor Brown, Boveri and Cie. AG, (1980) unpublished results.
12. A. G. EVANS, *Int. J. Fract.* **10** (1974) 251.
13. B. J. PLETKA, E. R. FULLER Jr and B. G. KÖPKE, in "Fracture Mechanics Applied to Brittle Materials" ASTM STP 678, edited by S. W. Freiman (American Society for Testing and Materials, Philadelphia, PA, 1979) pp. 19–37.
14. B. STALDER and H. H. KAUSCH, *J. Mater. Sci.* **17** (1982) 2481.
15. W. N. FINDLEY, in "Creep Characteristics of Plastics", Symposium on Plastics (American Society for Testing and Materials, 1944) p. 118.
16. A. C. MOLONEY, H. H. KAUSCH, T. KAISER and H. R. BEER, unpublished work.
17. H. R. BEER and T. KAISER, manuscript in preparation.

Received 23 October

and accepted 20 December 1985